Active Vibration Control of Delaminated Composite Plates Using Active fiber Patches as Actuators and Sensors

Abstract

This article presents a finite element investigation of transient behavior and active vibration control in a delaminated laminated composite plate equipped with an Active Fiber Composite (AFC) actuator. The deformation characteristics of both intact and delaminated sections are modeled using First-Order Shear Deformation Theory (FSDT). A numerical model incorporating a centrally positioned delamination is formulated and implemented in MATLAB using eight-noded serendipity elements with five degrees of freedom per node. The system's governing equations are derived via the principle of minimum total potential energy. An active velocity feedback control algorithm, defined by gain parameter (Gv), is applied to attenuate unwanted vibrations. Parametric analyses are performed to study the effects of boundary conditions, AFC patch location, delamination size, and feedback gain on the dynamic and frequency response of the composite plate.

Keywords: Active fiber composite, Delamination, First order shear deformation theory, Velocity feedback gain

1 Introduction

Active vibration control is always a challenging area for researchers. In modern era composite structures are extensively used in aircraft industries, marine engineering, sports industries and many more due to light weight and high strength to weight ratio. Piezoelectricactuators and sensors having large applications in vibration control and shape control of laminated structures. Delamination in the laminated composite structures is a common defect. Delamination occurs either due to presence of imperfection while fabrication (such as air entrapment or due to residual stresses) or application of fatigue loads during their service period of the structure. Due to delamination inlaminated composite structures there is degradation in stiffness of the structures. Many researchers have done the work in field of vibration analysis of delamination plates in early nineties [1, 2, and 3].

Tzou and Tseng [4] in 1989 proposed a new structure containing integrated distributed piezoelectric sensor and actuator where the distributed piezoelectric sensing layer monitors the structural oscillation due to direct piezoelectric effect and the distributed actuator layer suppresses the oscillation via the converse piezoelectric effect .Thus, the performance of plate model was evaluated. Hwang *et.al* [5] suggested a numerical solution and design strategy for a laminated composite plate with piezoelectric sensors or actuator where the vibration is controlled by passive and active control methods. Sun and Tong [6] in 2001 presented a novel approach for vibration control of smart plates using discretely distributed piezoelectric actuator and sensor and theresults obtained using the present optimal criteria. Lin and Nien[7] discussed adaptive modelling and shape control of laminate with piezoelectric actuators. The influence was studied for shape control under varying loads. The modelling and validation results show the reliability of the piezo-actuation for the shape control of laminated plates. In 2008 Ren [8]investigated the application of a piezoelectric actuator to control deformation of thin arbitrary lay-up composite laminates where a theoretical model based on Rayleigh–Ritz principle was developed to predict laminate cured shape and the effect of piezoelectric actuator layer.Dong *et.al* [9] focused on the study of the performance evaluation of an active vibration controller in a closed loop finite element (FE) environment for piezoelectric smart structures by integrating a reduced-order-model-based controller into the FE model where various numerical examples are presented to demonstrate the

efficiency of the proposed scheme for evaluating the vibration controller performance of piezoelectric smart structures in a closed loop FE environment. Fermi-Dirac distribution function employed with layer-wise theory in delaminated interface is described by Ghoshal*et.al* [10, 11]. They have deduced the transient response in presence of delamination at different interfaces of the laminate. Cho and Kim [12] are implemented the higher order zig-zag theory to study the static and dynamics behaviour of laminated plate with multiple delamination. They have determines the DOF in undelaminated region is independent of the number of layers and the number of delamination. The dynamic response of delaminated composite laminates and characterized according to the number of orientation of stacking sequence, mode shape and delamination size is discussed by Kim *et.al* [13]. They are used Layer-wise theory approached and compare their results with higher order theory. An improved Layer-wise theory is used in the transient analysis of delaminated plate [14]. Sohn and Kim [15] gave an active control algorithm was adopted, in order to recover the vibration characteristics of a delaminated composite structure, and control performances were numerically investigated where delamination of the laminated composite structure was modelled, using the improved layerwise theory. Khan and Kim [16] investigate the active vibration control of a piezo-bonded laminated composite in the presence of sensor partial debonding and structural delamination. They develop an electromechanically coupled finite-element model and analyze how these damage mechanisms influence the performance of a constant gain velocity feedback controller. Their results show that sensor debonding degrades vibration suppression, whereas structural delamination can enhance control authority due to reduced structural stiffness. Sharma et al. [17] investigated the static and free vibration behavior of smart curvilinear fiber laminated composite plates with delamination using a first-order shear deformation theory–based finite element model. Their study demonstrated that delamination significantly reduces structural stiffness and natural frequencies, while curvilinear fiber paths can mitigate this reduction by tailoring stiffness distribution. Additionally, the integration of piezoelectric actuators and sensors with active feedback control was shown to effectively suppress vibration in delaminated smart composite plates. Liu et al. [18] developed a theoretical and experimental framework for adaptive active vibration control of composite laminated plates using macro fiber composite (MFC) piezoelectric patches. By incorporating electromechanical coupling effects and implementing a filtered-x least mean square (FxLMS) algorithm, they demonstrated significant suppression of vibrations near natural frequencies as well as under multi-frequency and random excitations. Experimental and FEM validations confirmed the accuracy and effectiveness of the proposed adaptive closed-loop control system.

In this study Active Fiber Composite (AFC) actuators and sensors are used to control the undesirable vibratory responses. The Electro-mechanical formulation is based on first order shear deformation theory. The finite element analysis of bonded AFC patches on the surface of laminated plate along with delamination is developed and coded in MATLAB. The dynamic response is extracted by the help of Newmark's time integration scheme.

2 Mathematical formulation

The constitutive equations of Electro-Elastic relationship are given in Equation (1) and Equation (2).Whereas, Equation (1) corresponds to the in-plane stress-strain and shear stress-strain relationship and Equation (2) corresponds to the electro-mechanical-displacement due to AFC is expressed as follows,

$$\begin{Bmatrix}\sigma_{11}\\ \sigma_{22}\\ \sigma_{12}\end{Bmatrix}=\begin{bmatrix}Q_{11} & Q_{12} & 0\\ Q_{21} & Q_{22} & 0\\ 0 & 0 & Q_{66}\end{bmatrix}\begin{Bmatrix}\varepsilon_{11}\\ \varepsilon_{22}\\ \varepsilon_{12}\end{Bmatrix}-\begin{bmatrix}e_{11} & 0 & 0\\ e_{12} & 0 & 0\\ 0 & 0 & 0\end{bmatrix}\begin{Bmatrix}E_1\\ E_2\\ E_3\end{Bmatrix} \quad (1)$$

$$\begin{Bmatrix}\sigma_{23}\\ \sigma_{13}\end{Bmatrix}=\begin{bmatrix}Q_{44} & 0\\ 0 & Q_{55}\end{bmatrix}\begin{Bmatrix}\varepsilon_{23}\\ \varepsilon_{13}\end{Bmatrix}-\begin{bmatrix}0 & e_{42} & 0\\ 0 & 0 & e_{53}\end{bmatrix}\begin{Bmatrix}E_1\\ E_2\\ E_3\end{Bmatrix}$$

$$\begin{Bmatrix}D_1\\ D_2\\ D_3\end{Bmatrix}=\begin{bmatrix}e_{11} & e_{12} & 0 & 0 & 0\\ 0 & 0 & 0 & e_{43} & 0\\ 0 & 0 & 0 & 0 & e_{53}\end{bmatrix}\begin{Bmatrix}\varepsilon_{11}\\ \varepsilon_{22}\\ \varepsilon_{12}\\ \varepsilon_{23}\\ \varepsilon_{13}\end{Bmatrix}+\begin{bmatrix}\kappa_{11} & 0 & 0\\ 0 & \kappa_{22} & 0\\ 0 & 0 & \kappa_{33}\end{bmatrix}\begin{Bmatrix}E_1\\ E_2\\ E_3\end{Bmatrix} \quad (2)$$

Where, $\{\sigma_{ij}\}$ is the stress vector $[Q_{ij}]$ is the constitutive matrix, $\{\varepsilon_{ij}\}$ is the strain vector due to mechanical loading, $\{D_i\}$ is the electric displacement, $[e_{ij}]$ is the piezoelectric stress coefficient matrix, $[\kappa]$ is the dielectric constant, $\{E_i\}$ is the electric field vector.

If V is the electric potential difference between the two electrodes and h_{et} is the distance between two electrodes and we assume the electric field is acting along the X-direction so, the electric field vector can be written as,

$$\begin{Bmatrix}E_1\\ E_2\\ E_3\end{Bmatrix}=\begin{Bmatrix}-1/h_{et}\\ 0\\ 0\end{Bmatrix}V \quad (3)$$

In above equations (1-3), the constitutive relations are in material co-ordinate systems. Each lamina may have different orientations with respect to global or structural co-ordinate system; hence the co-ordinate transformation from the material coordinate system to the structural co-ordinate system is required. If the lamina is oriented at an angle θ with respect to the structural/global reference frame then the in-plane strain transformation matrix is given by

$$\begin{Bmatrix}\varepsilon_X\\ \varepsilon_Y\\ \varepsilon_{XY}\end{Bmatrix}=\begin{bmatrix}m^2 & n^2 & -2mn\\ n^2 & m^2 & 2mn\\ mn & -mn & m^2-n^2\end{bmatrix}\begin{Bmatrix}\varepsilon_{11}\\ \varepsilon_{22}\\ \varepsilon_{12}\end{Bmatrix} \quad (4)$$

Similarly shear strain transformation matrix is given by;

$$\begin{Bmatrix}\varepsilon_{YZ}\\ \varepsilon_{XZ}\end{Bmatrix}=\begin{bmatrix}m & -n\\ n & m\end{bmatrix}\begin{Bmatrix}\varepsilon_{23}\\ \varepsilon_{13}\end{Bmatrix} \quad (5)$$

Where $m=\cos\theta$ and $n=\sin\theta$

If the piezoelectric layers are oriented at angle θ_p with X-axis then piezoelectric stress coefficient matrix $[e]$ is transformed into $[e]_{xy}$ and can be presented as follows,

$$[e]_{xy} = \begin{bmatrix} m^2 & n^2 & 2mn \\ n^2 & m^2 & -mn \\ -mn & mn & m^2 - n^2 \end{bmatrix} [e] \begin{bmatrix} m & -n & 0 \\ -n & m & 0 \\ 0 & 0 & 0 \end{bmatrix} \quad (6)$$

Where $m=\cos\theta_{p\ and}$ $n=\sin\theta$

2.1 **Finite element formulation and stress resultant matrix for healthy plate element**

Element for a healthy (un-delaminated) platebased on the first order displacement theory is considered. An eight nodded serendipity element, with five degrees of freedom at each node is adopted here for element formulation. Displacement fields are interpolated using Lagrangian shape function as follows.

$$u_0 = \sum_{i=1}^{8} N_i u_i \ , \ v_0 = \sum_{i=1}^{8} N_i v_i \ , w_0 = \sum_{i=1}^{8} N_i w_i \ , \theta_x = \sum_{i=1}^{8} N_i \theta_{x_i} \ , \theta_y = \sum_{i=1}^{8} N_i \theta_{y_i} \quad (7)$$

Whereu_i, v_i, w_i are the nodal displacementsθ_{xi}, $\theta_{yi}$are nodal rotation degree of freedom along mid-plane and N_i is the shape function of corresponding node. Now strain-displacement relation is deriving from above equation.

$$\{\varepsilon\} = [\partial] \sum N_i \{\delta\} = \sum [\partial N_i] \{\delta\} \quad \text{Or} \quad \{\varepsilon\} = \sum [B_i] \{\delta\} \quad (8)$$

The stress-resultants can be obtained by integrating the stresses through the thickness of the laminate. The stress resultants due to mechanical loading is given by

$$\begin{Bmatrix} N_x \\ N_y \\ N_{xy} \\ M_x \\ M_y \\ M_{xy} \end{Bmatrix} = \begin{bmatrix} A & B \\ B & D \end{bmatrix} \begin{Bmatrix} \varepsilon_x \\ \varepsilon_y \\ \gamma_{xy} \\ k_x \\ k_y \\ k_{xy} \end{Bmatrix} \qquad [A_{ij}] = \sum_{k=1}^{N} \left[Q_{ij} \right]_k (z_k - z_{k-1})$$

$$[B_{ij}] = \frac{1}{2} \sum_{k=1}^{N} \left[Q_{ij} \right]_k (z^2{}_k - z^2{}_{k-1})$$

$$[D_{ij}] = \frac{1}{3} \sum_{k=1}^{N} \left[Q_{ij} \right]_k (z^3{}_k - z^3{}_{k-1}) \quad (9)$$

Where N_x, N_y, and M_x, M_y, are the normal forces and bending moment along X, Y axis whereas,$N_{xy}$and $M_{xy}$are in-plane shear force and twisting moment. $[A_{ij}]$=extensional stiffness matrix, $[B_{ij}]$ = extension-bending coupling matrix, $[D_{ij}]$ =bending stiffness matrix, $[Q_{ij}]_k$=constitutive stiffness matrix of lamina. Shear stress and strain relation in matrix form are as follows.

$$\begin{Bmatrix} Q_x \\ Q_y \end{Bmatrix} = k_{scf} \left[G_{ij} \right] \begin{Bmatrix} \gamma_{xz} \\ \gamma_{yz} \end{Bmatrix} \quad (10)$$

$$\left[G_{ij} \right] = \sum_{k=1}^{N} \begin{bmatrix} Q_{55} & Q_{45} \\ Q_{45} & Q_{44} \end{bmatrix} (Z_k - Z_{k-1})$$

Where Q_x and $Q_y$are the shear forces per unit length along XZ and YZ plane respectively. k_{scf}= shear correction factor (k_{scf}=5/6) and z = coordinate along depth and Z_k-Z_{k-1}=thickness of each lamina and Q_{44} , Q_{45} , Q_{55} modulus of rigidity. Laminated plate is divided into sub-laminate i.e. delaminated and healthy regions and analyzed separately. In Figure 1, 'abcd' is delaminated area of laminated plate, so the laminate is also split into upper delaminated sub-laminate and lower delaminated sub-laminate.

2.2 **Finite element procedure for Delamination modelling**

If a single delamination is present at the middle of the plate, then the upper and lower segment of the delaminated region is meshed separately. The coordinate system of delaminated segment is x^1, y^1, z^1. The z co-ordinate remains the same for the integral laminate as well as the delaminated sub-laminates, this way, we account for the eccentricities of the sub-laminate mid-planes with respect to the mid-plane of the integral laminate. So, according to the first order shear deformation theory, displacement field variable in the delaminated region is given below, similarly, for the sub-laminate displacement field is obtained by changing the subscript.

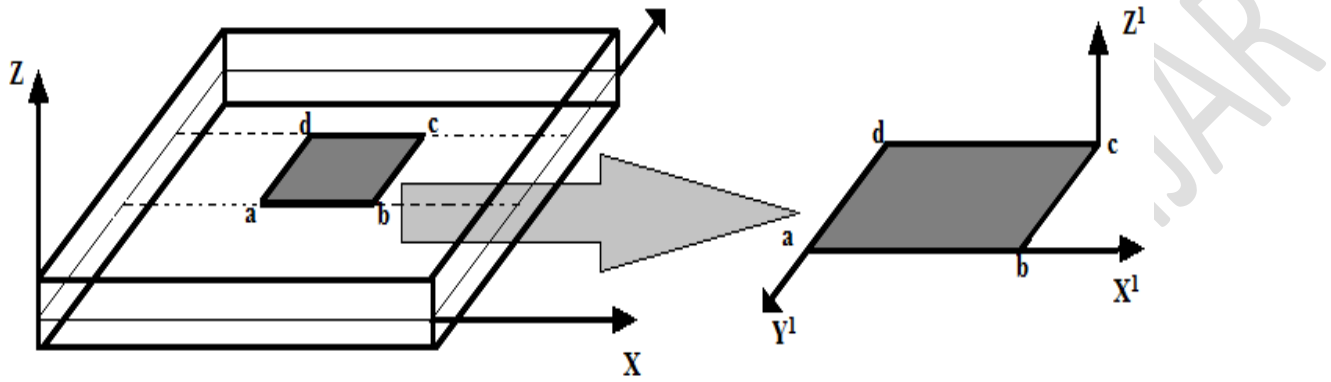

Fig.1. Isometric view of delaminated plate

$$
\begin{aligned}
u_B(x^1, y^1) &= u_B^0 + z\theta_{x_B} \\
v_B(x^1, y^1) &= v_B^0 + z\theta_{y_B} \\
w_B(x^1, y^1) &= w_B^0
\end{aligned}
\tag{11}
$$

If 'p' is the number of layers in the lower delaminated part and N is the total number of layers then the bending stiffness matrix and density matrix is changed according to Equation (12)

Lower delamination bending stiffness

$$
\begin{aligned}
[A_{ij}]_L &= \sum_{k=1}^{p} [Q_{ij}]_k (Z_k - Z_{k-1}) \\
[B_{ij}]_L &= \frac{1}{2} \sum_{k=1}^{p} [Q_{ij}]_k (Z^2{}_k - Z^2{}_{k-1}) \\
[D_{ij}]_L &= \frac{1}{3} \sum_{k=1}^{p} [Q_{ij}]_k (Z^3{}_k - Z^3{}_{k-1})
\end{aligned}
$$

Upper delamination bending stiffness

$$
\begin{aligned}
[A_{ij}]_U &= \sum_{k=p+1}^{N} [Q_{ij}]_k (Z_k - Z_{k-1}) \\
[B_{ij}]_U &= \frac{1}{2} \sum_{k=p+1}^{N} [Q_{ij}]_k (Z^2{}_k - Z^2{}_{k-1}) \\
[D_{ij}]_U &= \frac{1}{3} \sum_{k=p+1}^{N} [Q_{ij}]_k (Z^3{}_k - Z^3{}_{k-1})
\end{aligned}
\tag{12}
$$

$$
\begin{bmatrix} D_L \end{bmatrix} = \begin{bmatrix} A & B \\ B & D \end{bmatrix}_L \quad \text{And} \quad \begin{bmatrix} D_U \end{bmatrix} = \begin{bmatrix} A & B \\ B & D \end{bmatrix}_U
$$

From the above *A,B,D* matrices we have to calculate the D_L and D_U matrices for lower and upper delaminated segment element and then calculate the stiffness and mass matrix of delaminated element. The

stiffness and mass matrices calculations for the upper and lower sub-laminates will follow similar procedure as mentioned earlier for the healthy laminate.

2.3 **Dynamics analysis and control mechanism**

The kinetic energy of delaminated and healthy plate element and the total potential energy due to mechanical, electrical, mechanical external load and AFC (piezo-fiber) external load is given below.

$$T_p = \frac{1}{2}\sum_{L=2}^{n-1}\int_{\Omega}\{\varepsilon^L\}^T\{\sigma^L\}d\Omega + \frac{1}{2}\int_{\Omega}\{\varepsilon^1\}^T\{\sigma^1\}d\Omega - \frac{1}{2}\int_{\Omega}\{E^1\}^T\{D^1\}d\Omega$$
$$-\frac{1}{2}\int_{\Omega}\{\varepsilon^n\}^T\{\sigma^n\}d\Omega - \frac{1}{2}\int_{\Omega}\{E^n\}^T\{D^n\}d\Omega - \int_A\{\delta\}^T\{q\}dA - \int_A V_{z=h_n}\psi(x,y)dA \quad (13)$$

$$T_{KE} = \frac{1}{2}\sum_{K=1}^{N}\int_A\{\dot{\delta}\}^T[m]\{\dot{\delta}\}dA + \frac{1}{2}\sum_{K=1}^{P}\int_A\{\dot{\delta}_d\}^T[m]\{\dot{\delta}_d\}dA + \frac{1}{2}\sum_{K=P+1}^{N}\int_A\{\dot{\delta}_d\}^T[m]\{\dot{\delta}_d\}dA$$

Now applying the principle of minimum energy approach and substituting above equation in equation (13) we get three set of equilibrium equations with respect to nodal variable which are given as:

$$\begin{aligned}
&[M^e]\{\ddot{\delta}^e\} + [K^e_{dd}]\{\delta^e\} - [K^e_{da}]\{V^{en}\} - [K^e_{ds}]\{V^{e1}\} = \{F^e_1\}\\
&[K^e_{ad}]\{\delta^e\} + [K^e_{aa}]\{V^{en}\} = \{F^e_2\}\\
&[K^e_{sd}]\{\delta^e\} + [K^e_{ss}]\{V^{e1}\} = \{0\}
\end{aligned} \quad (14)$$

Where $[M^e]$ is the elemental mass matrix and $[k^e_{dd}]$, $[k^e_{aa}]$ and $[k^e_{ss}]$ are the elemental stiffness matrices due to mechanical displacements, the actuators and sensors potential respectively. $[k^e_{da}]$ and $[k^e_{ds}]$ are the electromechanical coupling stiffness matrices where subscript 'a' for actuator and 's' for the sensor. $\{F^e_1\}$ and $\{F^e_2\}$ are elemental mechanical force vector and elemental electrical force vector respectively. Now the global equilibrium equations are obtained after the assembling the equation (14) with respect to global axis.

$$\begin{aligned}
&[M\ ]\{\ddot{X}\} + [K_{dd}]\{X\} - [K_{da}]\{V_a\} - [K_{ds}]\{V_s\} = \{F_1\}\\
&[K_{ad}]\{X\} + [K_{aa}]\{V_a\} = \{F_2\}\\
&[K_{sd}]\{X\} + [K_{ss}]\{Vs\} = \{0\}
\end{aligned} \quad (15)$$

Where $[M]$ is the global mass matrices and $[K_{dd}]$, $[K_{aa}]$, $[K_{ss}]$, $[K_{da}]$, $[K_{ds}]$, $[K_{ad}]$, $[K_{sd}]$ are the global generalized stiffness matrices, $\{X\}$ is the global displacement and $\{F_1\}$ is the mechanical force vector, $\{F_2\}$ is the electric force vector. Eliminating $\{V_a\}$ and $\{V_s\}$ in Equation (15) can be rewritten as:

$$[M]\{\ddot{X}\} + [K^*]\{X\} = \{F_1\} + \{F_c\} \quad (16)$$

Where, $[K^*]$ and $\{Fc\}$ are the controlling stiffness and control feedback force. The detail control mechanism is given in Mahato and Maiti [21].

$$\begin{aligned}
&[K^*] = [K_{dd}] + [K_{da}][K_{aa}]^{-1}[K_{ad}] + [K_{ds}][K_{ss}]^{-1}[K_{sd}]\\
&\{F_c\} = [K_{da}][K_{aa}]^{-1}\{F_2\}
\end{aligned}$$

A Proportional- Derivative controller is used here and the voltage applied in actuator is given as below equation.

$$\{V_a\} = G_v\{\dot{V}_s\} \tag{17}$$

Newmark's time integration scheme [19, 20] is employed here for the calculation of dynamic response in time history. The frequency response is based on Discrete Fourier Transformation analysis. The details are given in references [21].

3 Result and Discussion

Numerical results are presented in this section is based on finite element code developed in MATLAB. The piezoelectric patches are integrated at the top and bottom of the plate. Electro-Mechanics is also incorporated into the finite element code developed for the piezoelectric patches. A parametric study on the effect of velocity feedback gain (G_v), piezoelectric patch location and boundary condition is carried out. The material properties of graphite/epoxy and AFC (piezoelectric) layer are shown in Table 1.

Table 1 Material properties of graphite/epoxy and AFC layer -50% fiber volume fraction.

Elastic module	graphite/epoxy [22]	AFC layer [23]
E_{11} (Gpa)	128	119.7
E_{22} (Gpa)	6.12	129.1
μ_{12}	0.3	0.35
μ_{13}	---	0.38
G_{12} (Gpa)	5.0	39.14
G_{13} (Gpa)	5.0	32.35
G_{23} (Gpa)	2.5	32.35
$e_{11}(c/m^2)$	---	14.14
$e_{21}(c/m^2)$	---	-3.34
$e_{24}(c/m^2)$	---	10.79
κ_{11}(F/m)	---	8.599×10^{-9}
κ_{33}(F/m)	---	6.485×10^{-9}
Density (Kg/m^3)	1600	6700

An asymmetric laminated square plate of dimension 0.6×0.6×0.006 m and orientation of each ply is (90/0/90/0) is taken for the analysis. A square delamination size 0.3×0.3 is present in middle of the laminate. The plate is divided into 8×8 mesh element. A point load of 1000N is applied at the middle of the plate (middle node). The analysis is carried out for the two boundary conditions *i.e.* simply supported boundary

condition (S-S-S-S) and cantilever boundary condition (C-F-F-F). Figure 2 shows the geometry of the plate and delamination location within the plate.

Figure 3 shows the piezoelectric patches position at different location on both side of plate. Here, four different location of patches position is discussed according to Liu et al. [24] for the dynamics analysis

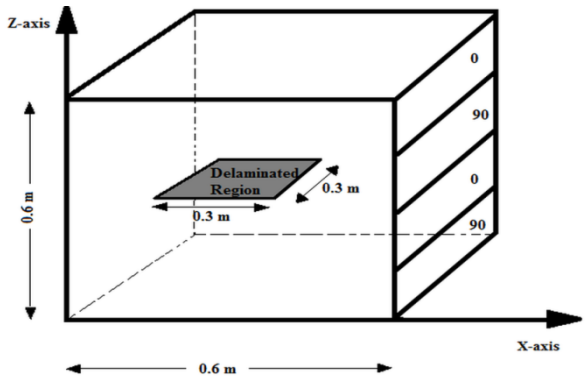

Fig. 2. Plate geometry and delamination location

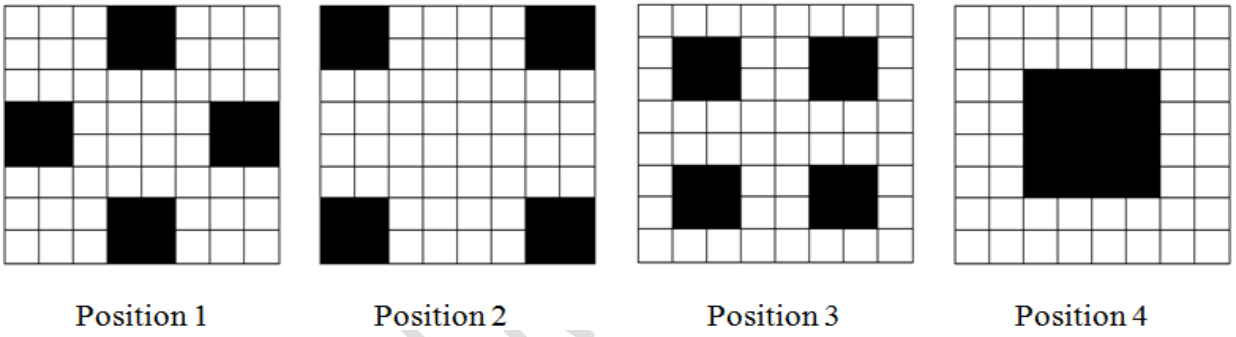

Fig. 3. AFC patches position at different places on plate

3.1 Vibration control of Delaminated plate

Vibration control of delaminated plate is studied in this section. Delamination causes a large transverse deflection as discussed earlier example, so vibration control is very much needed. A point load of 1000N is applied at the centre of the plate after giving an initial displacement, the load is suddenly removed and the plate is kept at vibration. A feedback system is activated at the mean time. The output voltage of the sensor layer is amplified by the amplifier and feedback to the actuator layer. Geometry and closed control loop system of the delaminated plate is shown in Figure 4.

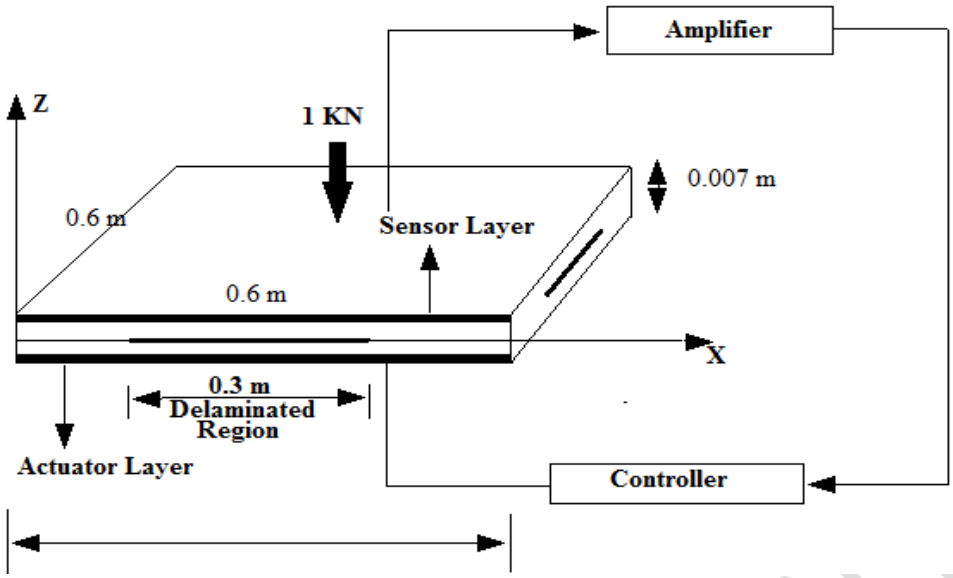

Fig. 4. Delaminated composite plate with feedback control loop system

Figure 5 shows the significant effect of the of piezoelectric patches position with respect to time and frequency. The velocity feedback gain (G_v) is taken 1 *i.e*G_v=1. It is clear from Figure 5 that the actuator sensor position 1 is the best location to control the transverse vibration. The analysis is done in S-S-S-S boundary condition.

Velocity feedback gain $G_v$is used to control the transverse deflection response in the following section. The values of G_v are varied from 0 to 5. When G_v= 0, AFC patches are not activated and so the response are remain unchanged throughout the time. The damping is induced by increasing the gain (G_v) from 0 to 5 so that the response comes to static state. In dynamic control system, the velocity feedback gain is always activating the damping of the system. In simply supported boundary condition the dynamic response with varying velocity feedback gain (G_v) value is shown in Figure 5, here the AFC patches position 1 is taken for the analysis. The time and frequency response of the delaminated plate is carried out corresponding to G_v=0, 1, 3, and 5 in Figure 6. The frequency response is illustrated here by the help of Fast Fourier Transformation (FFT). The higher peak has obtained for lower value of velocity feedback gain.

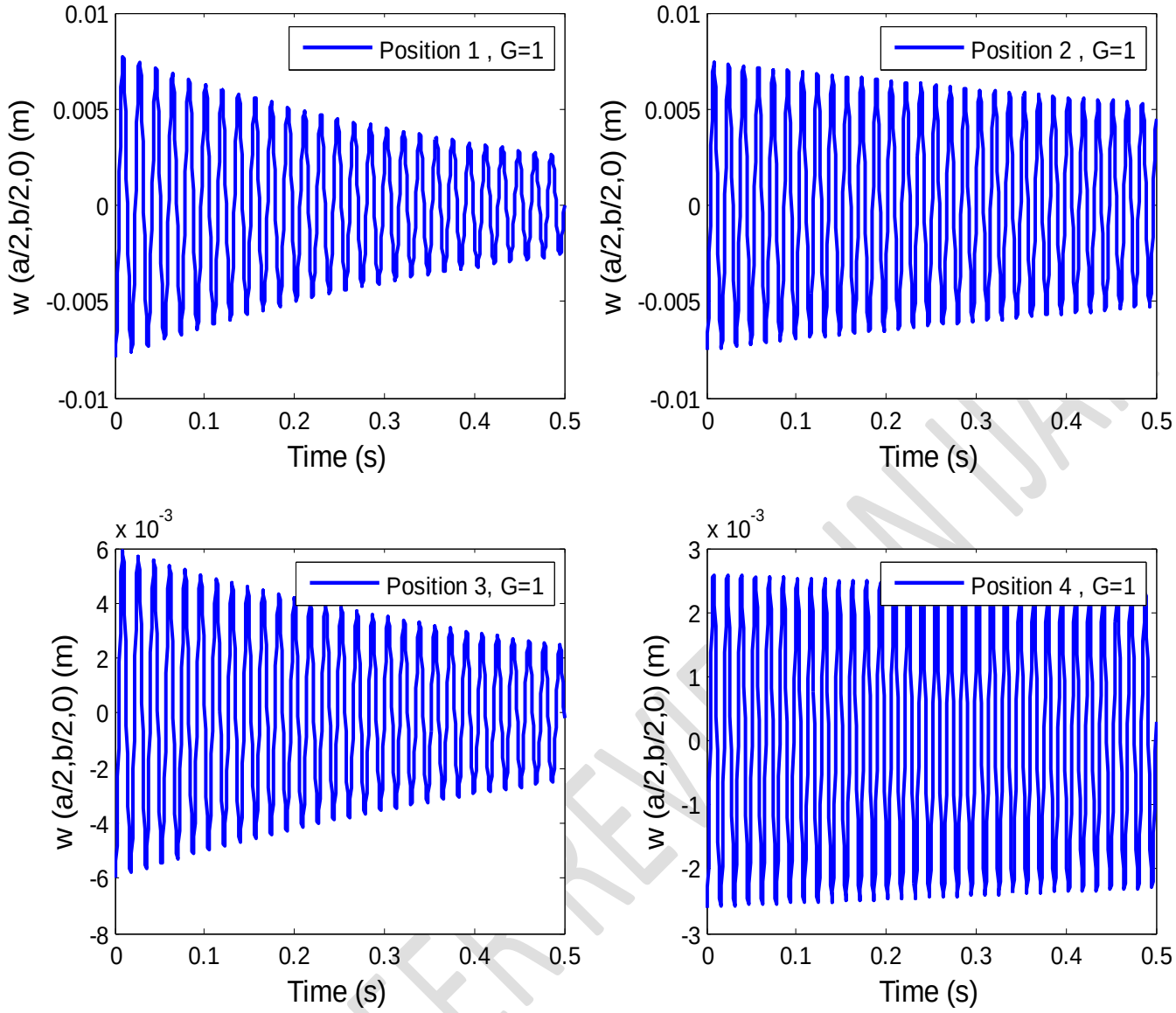

Fig. 5. Time response of delaminated plate at different location of AFC patches (G_v=1)

199

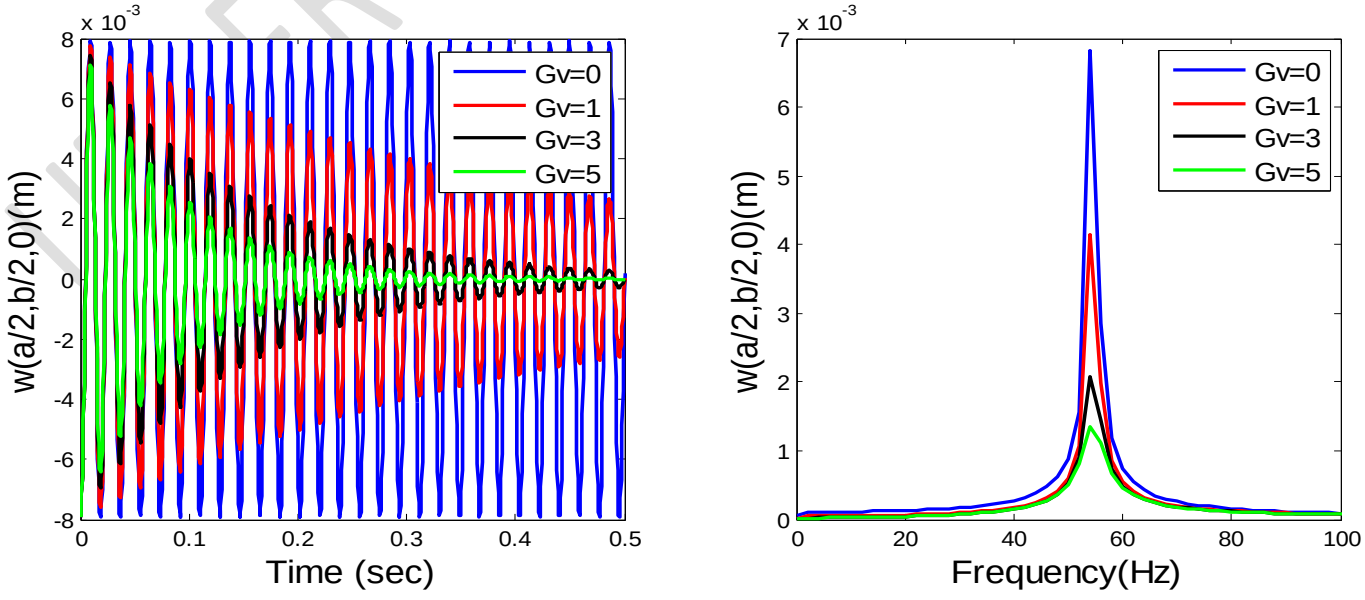

Fig. 6. Time and frequency response of simply supported delaminated plate in varying feedback gain (G_v)

In cantilever boundary condition the delaminated plate response with respect to time and frequency is shown in Figure 7. It is observed that the velocity feedback gain (G_v) is slightly increased to carrying the response in static state.

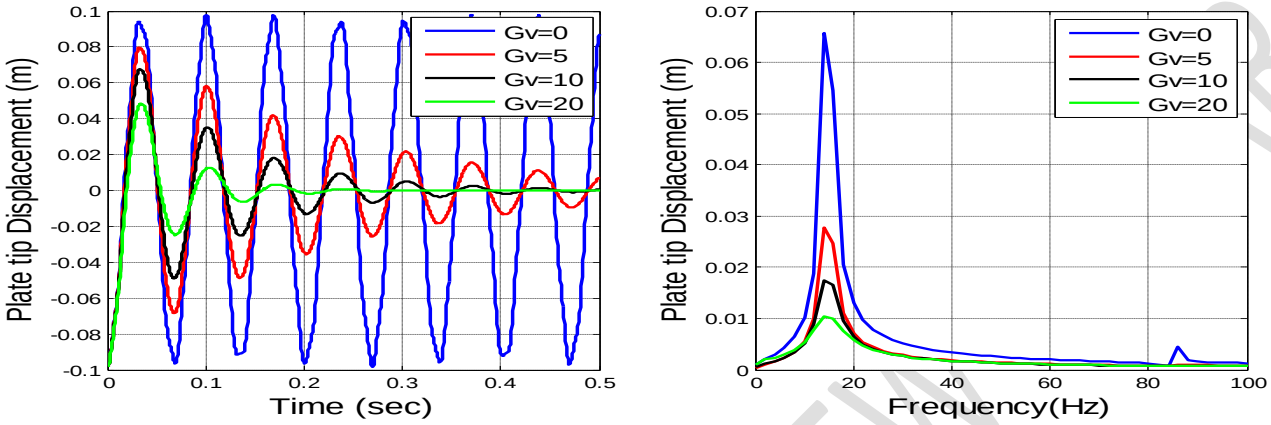

Fig. 7. Time and frequency response of cantilever delaminated plate in varying feedback gain (G_v)

It is clear from Figure 7 that in cantilever boundary condition the response is come to rest at 0.45 second when the G_v= 10, but when the value of $G_v$is increased from G_v= 10 to G_v= 20 it is taking 0.25 sec to come at rest. The frequency response of the delaminated plate in cantilever boundary condition is also show in Figure 7.

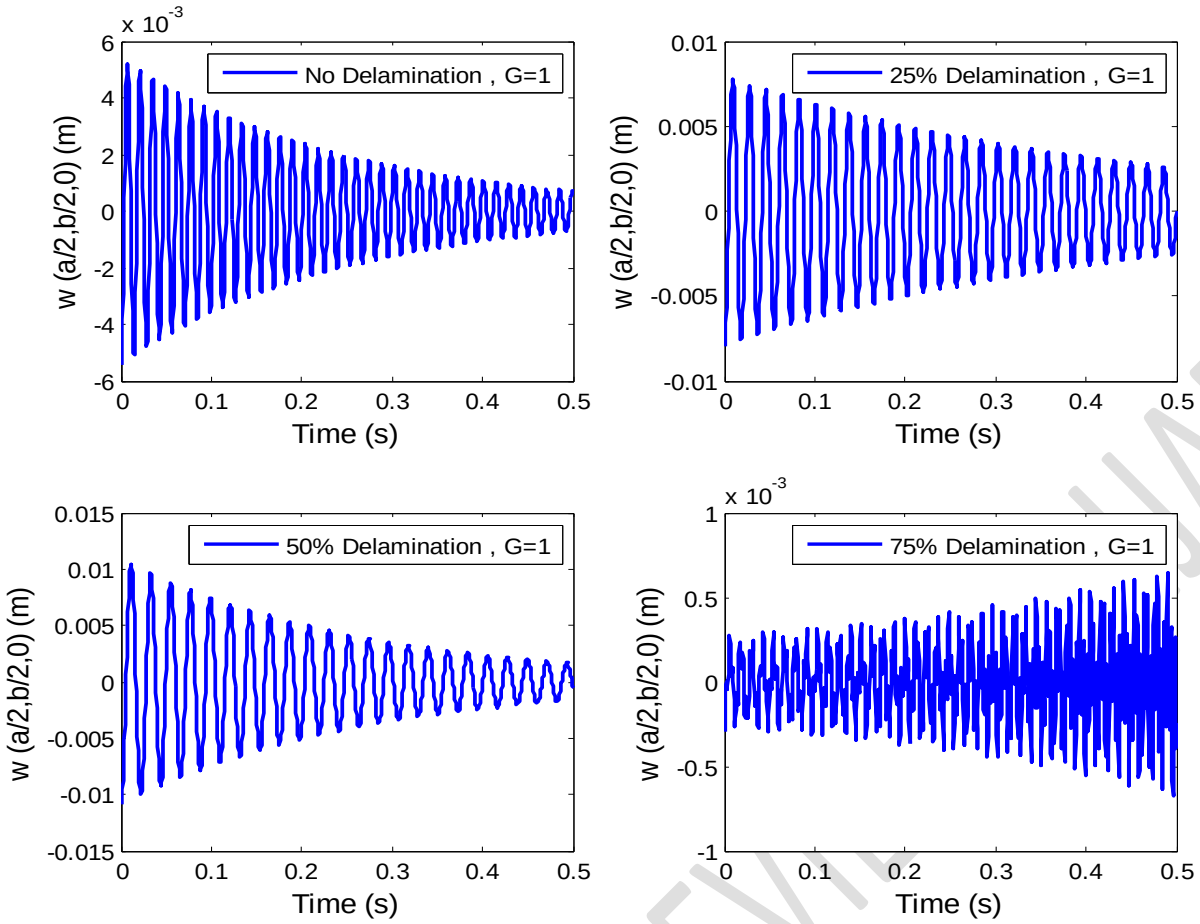

Fig. 8. Transient responses at various delaminated area in simply supported boundary (G_v=1)

The time response of maximum deflection at different mid-plane area delamination in simply supported boundary condition is shown in Figure 8. The piezoelectric patches position 1 (Fig 3) is taken here for the analysis. The velocity feedback gain is taken one here *i.e*(G_v= 1). It is seen from Figure 8 that the maximum deflection is 0.006m when no delamination is present, whereas maximum deflection is increased to 0.0136 m, 0.0201 m and 0.0482 m when mid-plane delamination is increased to 25%, 50% and 75% respectively. When 75% area is delaminated along the mid-plane of the plate, the time response is change rapidly, so the response is increase with increase in time. When 50% delamination is taken into consideration the time response is come to rest fast as compare to 25% area delamination.

Similarly the dynamics time response in cantilever boundary condition with different size of delamination is shown in Fig 9. The load of 1000 N is acting at the free end of the plate. The AFC patch position 1 (shown in Fig. 3) is taken.

The value velocity feedback gain is taken G_v=5. In this case, when the delamination size is increases, the response takes more time to come at static state. Delamination size is in form of area. When delamination size is 75% of the total area of plate, the dynamic response is abruptly increases with time similarly as in simply supported case. So it is clear from Fig. 8 and Fig. 9 that when delamination size is 75% of the total area of plate, the dynamic control is quite difficult.

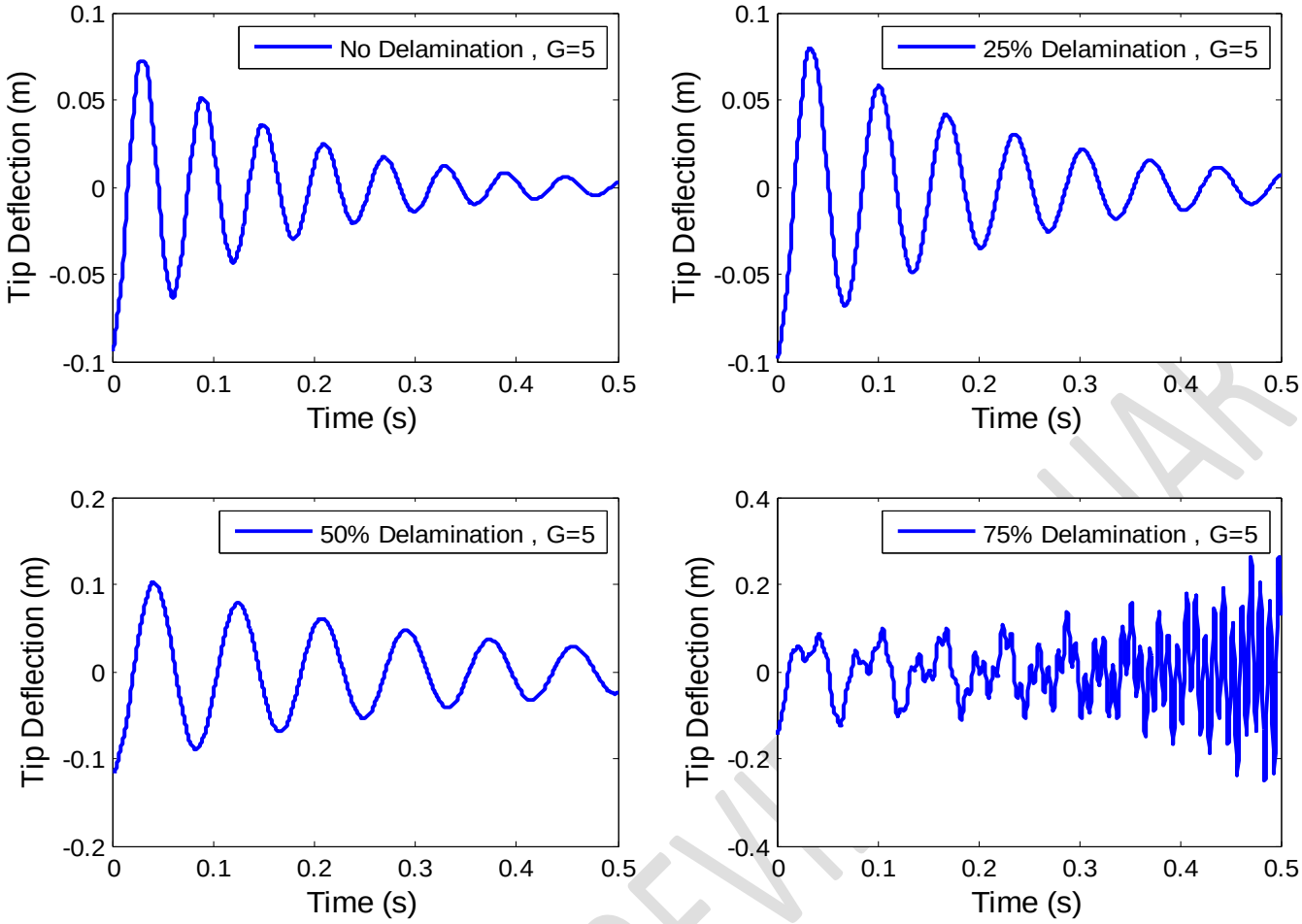

Fig. 9. Transient responses at various delaminated area in cantilever boundary (G_v=5)

4 Conclusion

A MATLAB based finite element code is developed for the control analysis of delaminated composite plates including piezoelectric (AFC) actuators sensors and feedback control loop. The numerical analysis of delaminated plate including control analysis is carried out in S-S-S-S and C-F-F-F boundary conditions. The transverse displacement has been deduced in delaminated and laminated plate. The dynamics response with varying velocity feedback gain (G_v) is carried out. The transient response of maximum deflection is extrapolated with different size of delamination. Some extensive conclusion are as follows:

- The effect of the AFC patches position (Fig. 3) is taken into consideration. It is observed from Figure 3 that when patches are away to delaminated region is good for structural control.
- The effective damping is induced due to velocity feedback loop to reduce the dynamics response. As the velocity feedback gain is increases the response come to rest faster.
- In cantilever boundary condition the value of $G_v$is greater than the simply supported boundary condition to carry the response in static state.
- The dynamic response of delamination plate having various size of delaminated area is carried out in both boundary condition *i.e.* S-S-S-S and C-F-F-F. It helps the designer that how much delamination is preferable.

5 References

[1]. Ju, F., Lee, H. P., & Lee, K. H. (1995). Finite element analysis of free vibration of delaminated composite plates. *Composites engineering*, *5*(2), 195-209.

[2]. Barbero, E. J., & Reddy, J. (1991). Modeling of delamination in composite laminates using a layer-wise plate theory. *International Journal of Solids and Structures*, *28*(3), 373-388.

[3]. Wang, J. T. S., Liu, Y. Y., &Gibby, J. A. (1982). Vibrations of split beams. *Journal of sound and vibration*, *84*(4), 491-502.

[4]. Tzou, H. S., & Tseng, C. I. (1990). Distributed piezoelectric sensor/actuator design for dynamic measurement/control of distributed parameter systems: a piezoelectric finite element approach. *Journal of sound and vibration*, *138*(1), 17-34.

[5]. Hwang, W. S., Hwang, W., & Park, H. C. (1994). Vibration control of laminated composite plate with piezoelectric sensor/actuator: active and passive control methods. *Mechanical Systems and Signal Processing*, *8*(5), 571-583.

[6]. Sun, D., Tong, L., & Wang, D. (2001). Vibration control of plates using discretely distributed piezoelectric quasi-modal actuators/sensors. *AIAA journal*, *39*(9), 1766-1772.

[7]. Lin, J. C., &Nien, M. H. (2007). Adaptive modeling and shape control of laminated plates using piezoelectric actuators. *Journal of Materials Processing Technology*, *189*(1-3), 231-236.

[8]. Ren, L. (2008). A theoretical study on shape control of arbitrary lay-up laminates using piezoelectric actuators. *Composite Structures*, *83*(1), 110-118.

[9]. Dong, X., Peng, Z., Ye, L., Hua, H., &Meng, G. (2014). Performance evaluation of vibration controller for piezoelectric smart structures in finite element environment. *Journal of Vibration and Control*, *20*(14), 2146-2161.

[10]. Ghoshal, A., Kim, H. S., Kim, J., Choi, S. B., Prosser, W. H., & Tai, H. (2006). Modeling delamination in composite structures by incorporating the Fermi–Dirac distribution function and hybrid damage indicators. *Finite elements in analysis and design*, *42*(8-9), 715-725.

[11]. Kim, H. S., Ghoshal, A., Kim, J., & Choi, S. B. (2006). Transient analysis of delaminated smart composite structures by incorporating the Fermi–Dirac distribution function. *Smart materials and structures*, *15*(2), 221.

[12]. Cho, M., & Kim, J. S. (2001). Higher-order zig-zag theory for laminated composites with multiple delaminations. *J. Appl. Mech.*, *68*(6), 869-877.

[13]. Kim, H. S., Chattopadhyay, A., &Ghoshal, A. (2003). Characterization of delamination effect on composite laminates using a new generalized layerwise approach. *Computers & structures*, *81*(15), 1555-1566.

[14]. Ghoshal, A., Kim, H. S., Chattopadhyay, A., & Prosser, W. H. (2005). Effect of delamination on transient history of smart composite plates. *Finite Elements in Analysis and Design*, *41*(9-10), 850-874.

[15]. Sohn, J. W., & Kim, H. S. (2015). Active recovery of vibration characteristics for delaminated composite structure using piezoelectric actuator. *International Journal of Precision Engineering and Manufacturing*, *16*(3), 597-602.

[16]. Khan, A., & Kim, H. S. (2019). Active vibration control of a piezo-bonded laminated composite in the presence of sensor partial debonding and structural delaminations. *Sensors*, *19*(3), 540.

[17]. Sharma, N., Swain, P. K., Maiti, D. K., & Singh, B. N. (2022). Static and free vibration analyses and dynamic control of smart variable stiffness laminated composite plate with delamination. *Composite Structures*, *280*, 114793.

[18]. Liu, T., Liu, C., & Zhang, Z. (2024). Adaptive active vibration control for composite laminated plate: theory and experiments. *Mechanical Systems and Signal Processing*, *206*, 110876.

[19]. Rubin, M. B. (2007). A simplified implicit Newmark integration scheme for finite rotations. *Computers & Mathematics with Applications*, *53*(2), 219-231.

[20]. Friberg, O. (1987). Jacobian matrices using the Newmark direct integration scheme. *Computers & structures*, *25*(2), 307-310.

[21]. Fisette, P., &Vaneghem, B. (1996). Numerical integration of multibody system dynamic equations using the coordinate partitioning method in an implicit Newmark scheme. *Computer Methods in Applied Mechanics and Engineering*, *135*(1-2), 85-105.

[22]. Shankar, G., Kumar, S. K., &Mahato, P. K. (2017). Vibration analysis and control of smart composite plates with delamination and under hygrothermal environment. *Thin-Walled Structures*, *116*, 53-68.

[23]. Mahato, P. K., &Maiti, D. K. (2010). Aeroelastic analysis of smart composite structures in hygro-thermal environment. *Composite structures*, *92*(4), 1027-1038.

[24]. Liu, G. R., Peng, X. Q., Lam, K. Y., &Tani, J. (1999). Vibration control simulation of laminated composite plates with integrated piezoelectrics. *Journal of sound and vibration*, *220*(5), 827-846.